sciendo

Journal of ELECTRICAL ENGINEERING, VOL 69 (2018), NO3, 226–232

Multilayer optical interconnects design: switching components and insertion loss reduction approach

Mohammad Reza Mokhtari, Hamed Baghban, Hadi Soofi *

The next generation of chip multi-processors point to the integration of thousands of processing cores, demanding high-performance interconnects, and growing the interest in optically interconnected networks. In this article we report on an interlayer silicon-based switch design that switches two channels simultaneously from an input waveguide into one of the two output ports. The introduced interlayer switch allows to design interconnects with previously unattainable functionality, higher performance and robustness, and smaller footprints with low insertion loss (< 1 dB), and high extinction ratio (> 18 dB). Interlayer switching combined with wavelength-routed and circuit-switched networks yield a low latency and low-loss interconnect architecture. Quantitative comparison between the proposed interconnect architecture and other reported structures in terms of loss, number of wavelengths and microring resonators reveals the proficiency of our design. For a 64-core interconnect implemented in 4 layers, the proposed architecture indicates an average loss reduction up to 42 % and 43 % with respect to single-layer lambda-router and GWOR.

K e y w o r d s: optical interconnect, interlayer switch, optical switching devices, ring resonator, silicon photonics

1 Introduction

As data rates to be processed spiral upwards, wiring electronics with photonics becomes increasingly an attractive solution to overcome the bottlenecks of electrical interconnects based on copper traces and wires. Although electrical transmission of data still dominates the short-reach interconnects, but with rising data rates and inherent limitations of electrical interconnects regarding bandwidth, latency and power consumption [1], gradually photonics makes a way into inter/intra chip communication. Optical interconnects with their compelling performance advantage pave a way to break these limitations with their notable high bandwidth, much lower latency, loss, and power consumption along with reduced interchannel crosstalk and electromagnetic interference [2]. Leveraging wavelength division multiplexing [3] can further enhance optical interconnects to herald approaching the challenging bandwidth of 1 Tbit/s, needed by multi-core central processor units in near future [4].

Silicon photonics [4, 5], compatible with CMOS technology and benefiting from the mature manufacturing technology in the silicon-based electronics, promises low-cost and highly integrated optical components such as optical interconnects. Optical switching is one of the vital required functionalities for optical interconnecting. An optical switch operates by selecting and redirecting an optical signal solely based on its wavelength. The switching wavelength can be either constant or tunable which corresponds to passive and active switches, respectively. In active switches, varying switching wavelength is realized by changing silicon's refractive index. Silicon due to its low electro-optic coefficient is not a suitable material for active photonic devices, although violating cases have been reported [6, 7]. Free carrier plasma dispersion effect is the most effective mechanism to change the refractive index in silicon. However, the weak index dependence on free carrier concentration [8] is very challenging and can increase the size of the system. Light-confining resonating structures with strong light confinement can overcome this limitation and enhance the effect of refractive index change on the transmission response [7].

According to utilized arbitration method, the proposed network-on-chips resorting to optical interconnects employ wavelength or circuit-switched networks for arbitration.

Briere *et al* have proposed a non-blocking contention-free passive router named λ-router which consists of 2×2 switches with the topology of Banyan network [9]. Generic wavelength-routed optical router (GWOR) compared with its previous non-blocking router designs, including the matrix-based crossbar, reduced crossbar and the λ-router, causes the lowest power loss and uses the least number of microring resonators [10]. As the GWOR and λ-router scale to support more IP cores, waveguide crossings are more and more introduced, incurring higher insertion losses. On the other hand, both λ-router and GWOR architectures have limited scalability by the number of wavelengths. As it is clear, the free spectral range (FSR), which is the length between two consecutive resonance peaks, determines the number of wavelength channels in a WDM system. The number of wavelength channels that can be transmitted concurrently at the same waveguide in a ring resonator based WDM interconnect is 62–64 [11,12]. To relieve these obstacles, one may employ inter-layer couplers to avoid waveguide crossings and

School of Engineering-Emerging Technologies, University of Tabriz, Tabriz 5166614761, Iran, h-baghban@tabrizu.ac.ir

DOI: 10.2478/jee-2018–0030, Print (till 2015) ISSN 1335-3632, On-line ISSN 1339-309X

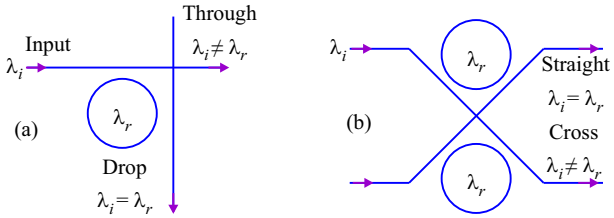

Fig. 1. Operation of a (a) – simple 1×2 ring resonator based switch, and (b) – 2×2 switch

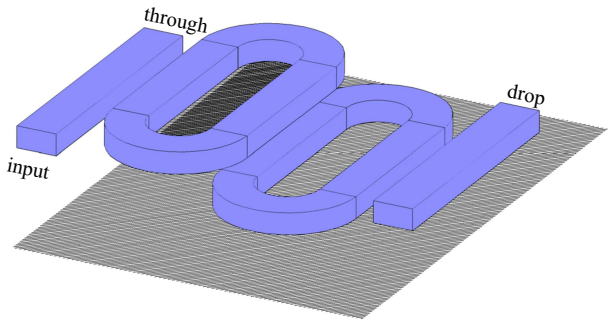

Fig. 2. Proposed vertically series-coupled racetrack resonators in two layers, side-coupled to waveguide buses

combine space division multiplexing with wavelength assignment, to reduce the limitation caused by the number of wavelengths [13]. An oblivious 5×5 wavelength-routed router has been presented in [14] which exhibits compact size and high on-chip bandwidth using multiple nanophotonic layers with torus topology. However, high design complexity makes it difficult to be extended to larger size networks. Although wavelength-routed passive networks (*eg* [9, 10, 13]) tend to provide a better power performance, low latency and contention-free communication, the constraint on the number of wavelength channels and waveguide crossings make implementing large-scale passive architectures a significant challenge.

A circuit-switched optical network with reconfigurable broadband optical switches has been proposed in [15] where data packet transmission requires setup and tear-down of an optical path, and these are carried out by employing an electrical packet-switched network, where each electrical router configures a ring resonator based optical switch to the 'on' or 'off' state. WANoC is another circuit switched network which efficiently reuses wavelengths [16]. However, once the setup packet reserves the path, there would be a high contention probability. Due to some enhancements in optical layer and centralizing the control logic in electrical layer, CWNoC architecture discussed in [17] presents much smaller latency and power consumption performance compared to the WANoC design. The electrical control network for optical circuit switching leads to network congestion, high latency due to path setup delay, and raised energy consumption but the overall system enjoys a good scalability.

The advent of the 3D stacking technology can reduce the on-chip communication delay and avoid serious implication for design complexity and power loss on a single layer due to waveguide crossing. Functional deposition of silicon photonics chips for multilayer photonic network-on-chips has been investigated recently where a 3D sculpting has been fabricated to stack optical devices in multiple silicon layers [18]. A multilayer silicon photonic micro-ring resonator filter, has been demonstrated using deposited silicon materials [19] and the feasibility of deposited silicon materials for multilayer photonic network-on-chips has been investigated [20]. MPNoC [21] is a 3D photonic interconnect which involves multiple layers to make a crossbar with no waveguide crossover. This architecture provides an ample bandwidth while it consumes more power compared to microring resonators in a similar structure called OCMP [22] due to silicon vias used for interlayer communication. There are several approaches for multilayer integration of optical interconnects [23, 24]. However, a prevalent way to connect optical layers vertically is using vertically coupled ring resonators [19, 25, 26]. Although 3D photonic on-chip interconnects for multicores has been introduced [26], no evaluation of the main switching block and characteristics of the whole network including switch size, and number of ring resonators has been reported.

In this article, we design an interconnect architecture employing both wavelength assignment and circuit-switched arbitration methods in order to benefit from the low latency and low power consumption of wavelength-routed passive networks along with high scalability of circuit-switched networks and hence, a moderate performance. The proposed multilayer topology leverages an interlayer reconfigurable switch based on two vertically cascaded microring resonators to take advantage of multi-band response and reduced switching loss. Wavelength-routed network realizes intra-layer communication between IP cores in each layer while the inter-layer communication is done by switching on the inter-layer switches.

The interlayer switch design and characteristics will be further discussed and the system-level performance of the optical interconnect will be analyzed.

2 Interlayer switch design

The operations of a simple ring-resonator-based and a double ring-based switches are schematically illustrated in Fig. 1, implementing 1×2 and 2×2 switching functions in Figs. 1(a) and 1(b), respectively. The input signal is coupled to the drop port provided that the input wavelength matches one of the resonance wavelengths of the microring resonator and satisfies the equation $m\lambda = n_{\text{eff}}L$, with L being the length of the resonating cavity n_{eff} the effective index of the resonant mode, and m being an integer [27]. The geometry and the material of the waveguide determine the effective index of the resonant mode. The state of the switch can be manipulated by charge carrier control where the change in

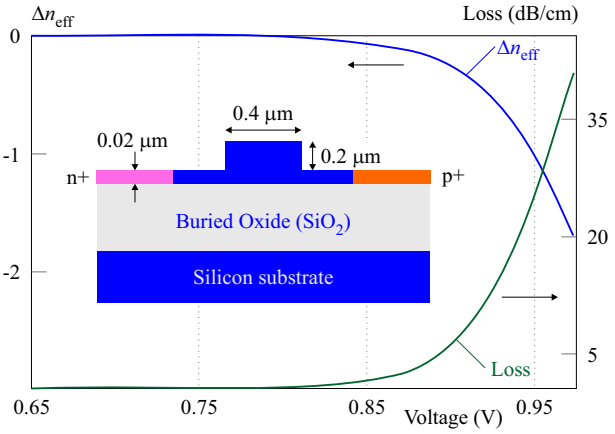

Fig. 3. Simulated carrier injection-induced effective index change (blue curve) and loss (red curve) as functions of the driving voltage. Inset: cross-sectional view of the lateral p-i-n junction straddled across a silicon waveguide

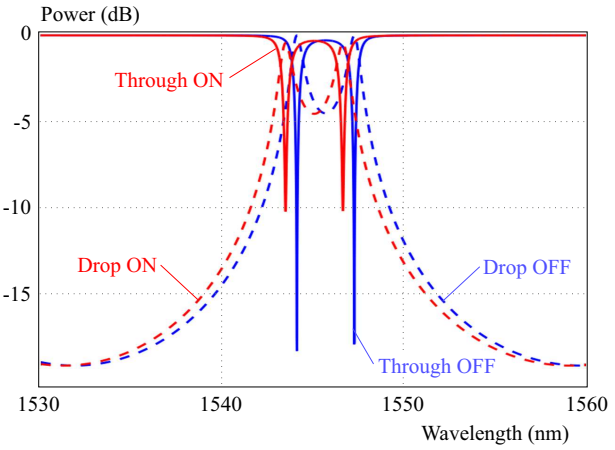

Fig. 4. Simulated off-state (blue) and on-state (red) transmission response at the through- (solid curves) and drop-ports (dashed curves)

carrier concentration alters the effective index and consequently resonant wavelength of the ring. Thus, a refractive index change of $\Delta n \sim 2 \times 10^{-3}$ with injection or depletion of 10^{18}carriers/cm^3 can be produced. The induced variations in real refractive index and optical absorption coefficient by carrier concentration variation at $1.55\,\mu$m is given by

$$\Delta n = -\left[8.8 \times 10^{-22}\Delta N + 8.5 \times 10^{-18}(\Delta P)^{0.8}\right], \quad (1)$$

$$\Delta \alpha = -\left[6.0 \times 10^{-18}\Delta P + 8.5 \times 10^{-18}\Delta N\right] \quad (2)$$

where ΔN and ΔP (cm^{-3}) are the electron and hole concentration change, respectively. Switching operation and carrier concentration variation can be realized using a p-n junction. Figure 2 outlines the configuration of the proposed interlayer switch. Upper layer consists of a waveguide coupled to a resonator which is vertically coupled to another resonator in the lower layer. The vertically coupled resonators have a transmission response similar to series coupled resonators in a single layer. The resonant mode can then couple to the drop port provided that the input signal meets the resonance condition. Otherwise, the input signal will pass a straight path on the same waveguide, without altering the layer.

High order resonator structures such as coupled ring resonator optical waveguides (CROWs) are required to reach and handle high data rates [28–30] . Cascading ring resonators increases the filters selectivity and makes drop channels extremely fine with steeper sidewalls. Sharper rolloff and flatter passbands makes the transfer function of these structures superior to single-ring structures and therefore, avoiding degraded extinction ratio when the resonator bandwidth is widened [30] . Broadband/multiband coupled microring resonators, capable of transmitting several wavelength channels simultaneously can reduce the number of microring resonators. The proposed switch is capable of switching two wavelength channels simultaneously in a FSR.

The inter-layer switch passes specific wavelength channels in the 'off' state on a single layer while in the 'on' state transmits those channels to its drop port located on a neighboring optical layer. Implementing both of these functions requires devising a scheme for wavelength shift. The shift in transmission response is provided by varying the carrier concentration in the resonators' waveguide. A lateral p-i-n diode, which is wrapped around microring resonators, is used for carrier injection. The cross section of the resonators' waveguide is shown in Fig. 3. By tuning the effective index of the ring waveguide, the resonance frequency and transmission response is modified. The effective index of the ring is modulated electrically by injecting free carriers using a forward biased p-i-n junction embedded in the microring resonator. The inset in Fig. 3 shows the cross section of the simulated lateral p-i-n junction straddled across the silicon waveguide.

Both the waveguide forming the ring and coupling to the ring resonator have width of 400 nm and height of 220 nm. The p-i-n diode has an intrinsic region width of $1\,\mu$m. Ohmic contacts are deposited on the highly doped p and n regions, whose concentrations are 2×10^{19}cm^{-3}, and 1×10^{20}cm^{-3}. The highly doped regions are formed $0.3\,\mu$m away from the edge of the waveguide to reduce their interaction with the waveguide mode evanescent field and hence minimize the light scattering loss. Silicon-on-insulator (SOI) substrate is assumed for the waveguide. A $1\,\mu$m-thick layer of silicon dioxide is deposited to cover the waveguide as a cladding layer. Fig. 3 shows the simulated carrier injection-induced effective index change (solid curve) and loss (dashed curve) as functions of the driving voltage. The higher free carrier concentration drops the effective index and induces a higher free carrier absorption, raising the 'on'-state drop-port transmission loss along with wavelength blue shift. The diameter of the ring is $15\,\mu$m and the gap between the straight waveguide and the ring is 50 nm. To ensure high coupling coefficient between the waveguide and the ring, racetrack resonators are used to increase the coupling length and hence the coupling factor. The electron-hole pair density in the cavity increases as the forward bias on the p-i-n

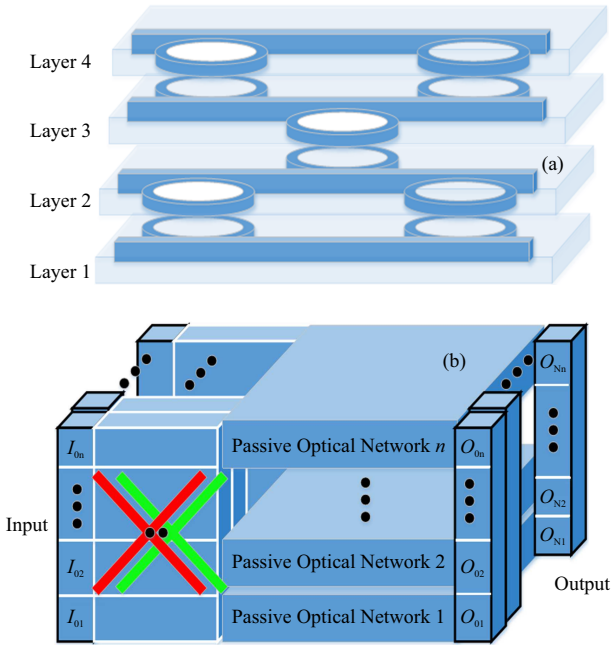

Fig. 5. (a) – ascending and descending path for vertical signal transmission through interlayer switches, this ILS set supports down/up-stream data transmission for four wavelengths channels, and (b) – proposed multi-layer optical interconnect with inter-layer communication handled by ILS sets shown by crosses

diode increases. The structure can be modeled by transfer matrix method and using the electrical and optical simulation results. The red and blue curves in Fig. 4 show the spectra when the bias voltages of 0.95 and 0 are applied to the p-n diode. The injection of carriers in the cavity increases effective index and blue shifts the resonance. Owning to the increased optical absorption, the depths of the notches in the spectra decreases. The extinction ratio for the through and drop ports at the driving voltage of 0.95 are about 17.5 dB and 5 dB, respectively. The FSR width is 28.5 nm and with a forward bias voltage of 0.95 the spectrum blue-shifts 0.63 nm.

3 System level performance and assessment

To utilize the advantage of a multilayer interconnect we have proposed interlayer switches (ILS) in Section 2. Different optical layers can be unified by a set of ILSs. By electrical contacts provided for each ILS, the set can be tuned to required reconfiguration and hence all the corresponding inputs in different layers can connect to each other. The approach taken here is to locate interlayer switches between optical layers diagonally. As it is shown in Fig. 5(a) a complete communication requires two separate paths. The ascending path is used for upstream data packets, which are heading to the upper layers, while the descending path transmits downstream signals to the lower layers. As mentioned before each switch can handle switching of four wavelength channels (two at the 'on' and two at the 'off' state, Fig. 4.) so interlayer transmission of every four wavelength channels requires a distinct set of ILS operating at the corresponding wavelengths. A $64 \times 64\lambda$-router implemented in 4 layers for example, requires 16 wavelength channels in each layer and hence 4 interlayer switching sets to connect corresponding inputs at different layers. Passive networks designed by wavelength assignment are stacked over each other. The number of layers that can be deposited depends on the fabrication technology. A distinct wavelength channel is assigned for each input-output pair in each layer, and all the deposited passive networks have the same design. To route a signal from I_{n1} (nth input in the first layer) to O_{ml} (mth output in the lth layer) the input signal is modulated with the assigned wavelength for I_n–O_m pair. The modulated signal is vertically directed to the lth layer through the configured set of interlayer switches, and the destination network once receiving the signal will passively route it to the output port. The interlayer communication is accomplished without any need for wavelength conversion and despite using the same wavelength channels at different layers, contention-free intra-layer communication is guaranteed. All the corresponding inputs in multilayer architecture are connected to an interlayer switching block as it is depicted in Fig. 5(b). Each block contains multiple sets of ILS, and each set handles four wavelength channels, which is shown by a colorful cross.

Interlayer switching is accomplished by circuit-switching methodology. The optical path is reserved before the optical data is transmitted through interlayer switches. Processing node first send transmission request to the network arbiter logic, the path allocation occurs, and the path is reserved for signal transmission. If the intended vertical path or one of the inter-layer switches is already handling another operation, the transmission had to be postponed until the path tears down.

Here, we compare two existing passive optical interconnects, the λ-router and GWOR, with their multi-layered counterparts. The aspects to consider are the maximum and average insertion loss, the number of wavelengths and microring resonators used.

The constraint on the number of wavelengths that can be multiplexed in one waveguide limits the scalability of passive optical interconnects. Therefore, wavelength resources must be efficiently utilized. Inherent advantage of multi-layer networks can push back the limitations set by restricted wavelength resources. The number of wavelengths used in λ-router and GWOR are N and $N-1$ for a single layer $N \times N$ router, respectively [9, 10]. This means that the number of wavelengths increases linearly as the size increases. Therefore, the scalability is limited when the number of wavelengths reaches the boundary. Chen *et al* have been addressed this challenge using space division multiplexed based cells (SBCs) [13].

The larger the size of these cells, the more times the same wavelength can be reused in different waveguides, thus fewer number of wavelengths will be used at the cost of more consumed waveguide and occupied area [13].

Table 1. Number of microring resonators required for modulation and detection in the λ-router and GWOR

Switch size	Number of layers			
	1	2	4	8
8×8	112			
16×16	480	224		
32×32	1984	960	448	
64×64	8064	3968	1920	896

Table 2. Number of microring resonators required for routing and vertical switching in the λ-router and GWOR for various number of layers

Switch size	Number of layers			
	1	2	4	8
8×8	48			
16×224	128			
32×32	960	578	384	
64×64	3968	2342	1664	832

3D optical interconnects inherently address this issue since the cores in different layers can use the same wavelength independently and the limitation on the number of wavelengths only imposes each layer separately.

Another aspect for evaluation of optical interconnects is the number of required microring resonators. Optical interconnect networks evaluated here are non-blocking structures, which means that network prevents any self-communication between any input-output pairs. Therefore, for an $N \times N$ λ-router and GWOR, there exist $N-1$ possible destination for each input. Considering the directly coupled input-output pairs through the waveguide, an $N \times N$ interconnect needs $N \times (N-2)$ microring resonators for optical interconnection. Table 1 lists the number of required microring resonators for the single and multi-layer interconnects. The number of microring resonators increases exponentially as the structure scales up for a single-layer interconnect. In contrast, when the passive optical networks are duplicated in multiple stacked layers, scaling the structure up is accomplished through addition of extra layers therefore the number of passive ring resonators increases linearly as the structure scales up. The number of passive microring resonators becomes less than half of the previous single layer structures by doubling the layers in a multi-layer interconnect. An m-layer $N \times N$ interconnect also requires $2 \times q \times \lceil N/m \rceil \times \lceil N/4m \rceil \times (m-1)$ ring resonators for interlayer switching, where the $\lceil\ \rceil$ notation denotes the ceiling function, and q is 1 for two-layer architecture and is 2 for architectures with more layers.

As shown in Tab. 2, the number of microring resonators used for modulation and detection becomes significantly fewer by increasing the layers. In a single-layer architecture, $2\times(N\times N-1)$ ring resonators are required for modulation and detection since a distinct wavelength channel is assigned for each input-output pair. An m-layer $N\times N$ interconnect consists of m, $\lceil N/m \rceil \times \lceil N/m \rceil$ layers, hence, the required microring resonators for modulation and detection is $2m \times \lceil N/m \rceil \times (\lceil N/m \rceil - 1)$.

Therefore, there is a considerable decrease in the number of microring resonators for multi-layer structures. Although the scheme presented in [13] requires 195,840 microring resonators for a 256×256 optical interconnect, our proposed scheme needs only 109056 microring resonators by implementing a 256×256 optical interconnect in four 64×64-layers which means $\sim 44\,\%$ reduction in the number of microring resonators.

Another obstacle for the scalability and feasibility of the optical interconnects is their insertion loss. The total power loss (P_T) experienced by an optical signal can be estimated by

$$P_T(i,j) = 1.5 \sum P_D + 0.01 \sum P_{\mathrm{TH}} + 0.05 \sum P_C + 0.013 \sum P_B + \sum P_{IL} \quad (3)$$

where the loss contributions are: P_D – drop, P_{TH} – through, P_C – crossing, P_B – bending, and P_{IL} – interlayer, respectively.

All the power loss parameters and assumptions are adopted from [12] for our calculations. Each ring resonator has a resonance power-drop loss of 1.5 dB, a through loss of 0.01 dB, and a crossing and waveguide bending losses of 0.05 dB and 0.013 dB, respectively. Each interlayer coupler has a 1 dB loss. Figures 6 and 7 show the maximum and average estimated power loss experienced by an optical signal traversing a λ-router and GWOR of varying sizes and layer numbers. The figures include the results of previously proposed single layer interconnects and their multilayer implementation with the scheme proposed in this article. Data traffic distribution is assumed such that any input port can connect to any output port with equal probability. As we scale the size up, the reduction in insertion loss becomes more and more obvious. This reduction is due to eliminating unnecessary crossings from the optical interconnect. Although multilayer interconnection eliminates unnecessary crossings, however, this does not necessarily mean that the more number of layers will induce smaller insertion loss. Since each interlayer switching causes 1dB loss, splitting the network into multiple layers is profitable only when the aggregate reduction in unnecessary crossing loss is more than increase in interlayer transmission loss.

That is why four-layer implementation of 64×64 interconnect has the minimum average insertion loss according to Fig. 6. It can be inferred from Fig. 6 and Fig. 7 that four-layer architecture has an optimum number of layers for a 64×64 interconnect since it reduces the average and maximum insertion loss by 43 % and 44 % compared to single layer GWOR, and by 42 % and 5.5 % compared to λ-router.

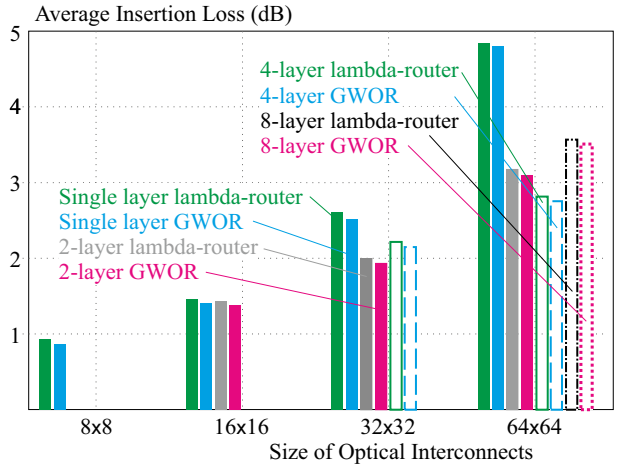

Fig. 6. The average insertion loss in different optical interconnects

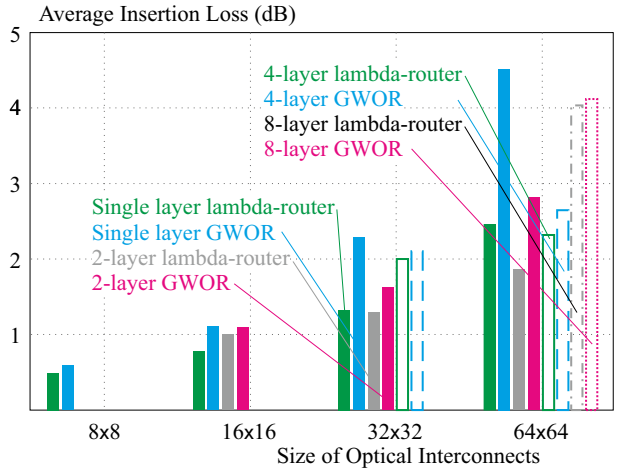

Fig. 7. The maximum insertion loss in different optical interconnects

4 Conclusion

Based on an interlayer switching scheme, an optical interconnect architecture was introduced in this report. Such interlayer switches can be readily used along with single layers of wavelength routed interconnects, moving them toward the ability to harness optical power and space efficiently on a chip. The more the coupled rings in the interlayer switch, the more the stability to thermal variation, and the better and finer the transmission response. The comparison results show that a 64×64 interconnect in 4 layers reduces the number of microring resonators by $\sim 70\,\%$ and the average and maximum insertion loss by $43\,\%$ and $44\,\%$ compared to single layer GWOR, and by $42\,\%$ and $5.5\,\%$ compared to λ-router.

References

[1] D. A. Miller, "Optical Interconnects to Electronic Chips", *Applied Optics*, vol. 49, 2010, pp. F59–F70.

[2] D. A. Miller, "Rationale and Challenges for Optical Interconnects to Electronic Chips", *Proceedings of the IEEE*, vol. 88, 2000, pp. 728–749.

[3] I. O'Connor and G. Nicolescu, *Integrated Optical Interconnect Architectures for Embedded Systems*, Springer Science & Business Media, 2012.

[4] C. Gunn, "CMOS photonics for high-speed interconnects", *IEEE Micro*, vol. 26, 2006, pp. 58–66.

[5] G. T. Reed, G. Mashanovich, F. Gardes and D. Thomson, "Silicon Optical Modulators", *Nature photonics*, vol. 4, 2010, pp. 518–526.

[6] A. Liu, R. Jones, L. Liao, D. Samara-Rubio, D. Rubin, O. Cohen *et al*, "A High-Speed Silicon Optical Modulator based on a Metal-Oxide-Semiconductor Capacitor", *Nature*, vol. 427, 2004, pp. 615–618.

[7] Q. Xu, B. Schmidt, S. Pradhan and M. Lipson, "Micrometre-Scale Silicon Electrooptic Modulator", *Nature*, vol. 435, 2005, pp. 325–327.

[8] R. A. Soref and B. R. Bennett, "Electrooptical effects silicon", *IEEE Journal of Quantum Electronics*, vol. 23, 1987, pp. 123–129.

[9] M. Briere, B. Girodias, Y. Bouchebaba, G. Nicolescu, F. Mieyeville, F. Gaffiot *et al*, "System Level Assessment of an Optical NoC an MPSoC Platform", *Proceedings of the conference on design, automation and test*, Europe, 2007, pp. 1084–1089.

[10] X. Tan, M. Yang, L. Zhang, Y. Jiang and J. Yang, "A Generic Optical Router Design for Photonic Network-on-Chips", *Journal of Lightwave Technology*, vol. 30, 2012, pp. 368–376.

[11] K. Preston, N. Sherwood-Droz, J. S. Levy, and M. Lipson, "Performance Guidelines for WDM Interconnects based on Silicon Microring Resonators", *CLEO: Science and Innovations*, 2011, p. CThP4.

[12] C. Batten, A. Joshi, J. Orcutt, A. Khilo, B. Moss, C. Holzwarth *et al*, "Building Manycore Processor-to-Dram Networks with Monolithic Silicon Photonics", *High Performance Interconnects*, 2008. HOTI'08. 16th IEEE Symposium on, 2008, pp. 21–30.

[13] K. Chen, H. Gu, Y. Yang and D. Fan, "A Novel Two-Layer Passive Optical Interconnection Network for On-Chip Communication", *Journal of Lightwave Technology*, vol. 32, 2014, pp. 1770–1776.

[14] N. Kirman and J. F. Martínez, "A Power-Efficient All-Optical On-Chip Interconnect Using Wavelength-Based Oblivious Routing", *ACM Sigplan Notices*, 2010, pp. 15–28.

[15] A. Shacham, K. Bergman and L. P. Carloni, "Photonic Networks-On-Chip for Future Generations of Chip Multiprocessors", *IEEE Transactions on Computers*, vol. 57, 2008, pp. 1246–1260.

[16] Z. Chen, H. Gu, Y. Yang and K. Chen, "Low Latency and Energy Efficient Optical Network-On-Chip using Wavelength Assignment", *IEEE Photonics Technology Letters*, vol. 24, 2012, pp. 2296–2299.

[17] Z. Chen, H. Gu, Y. Yang and D. Fan, "A Hierarchical Optical Network-On-Chip Using Central-Controlled Subnet and Wavelength Assignment", *Journal of Lightwave Technology*, vol. 32, 2014, pp. 930–938.

[18] P. Koonath and B. Jalali, "Multilayer 3-D Photonics Silicon", *Optics Express*, vol. 15, 2007, pp. 12686–12691.

[19] A. Biberman, N. Sherwood-Droz, X. Zhu, K. Preston, G. Hendry, S. Levy *et al*, "Photonic Network-On-Chip Architecture Using 3D Integration", *SPIE OPTO*, 2011, pp. 79420M–79420M-4.

[20] A. Biberman, K. Preston, G. Hendry, N. Sherwood-Droz, J. Chan, S., Levy *et al*, "Photonic Network-On-Chip Architectures Using Multilayer Deposited Silicon Materials for High-Performance Chip Multiprocessors", *ACM Journal on Emerging Technologies Computing Systems (JETC)*, vol. 7, 2011, p. 7.

[21] X. Zhang and A. Louri, "A Multilayer Nanophotonic Interconnection Network for On-Chip Many-Core Communications", *Proceedings of the 47th Design Automation Conference*, 2010, pp. 156–161.

[22] R. W. Morris, A. K. Kodi, A. Louri and R. D. Whaley, "Three-Dimensional Stacked Nanophotonic Network-On-Chip Architecture with Minimal Reconfiguration", *IEEE Transactions on Computers*, vol. 63, 2014, pp. 243–255.

[23] P. Carloni. P. Pande and Y. Xie, "Networks-On-Chip Emerging Interconnect Paradigms: Advantages and Challenges", *Proceedings of the 2009 3rd ACM/IEEE International Symposium on Networks-on-Chip*, 2009, pp. 93–102.

[24] L. Ramini, P. Grani, D. S. Bartolini and D. Bertozzi, "Contrasting Wavelength-Routed Optical NoC Topologies for Power-Efficient 3D-Stacked Multicore Processors using Physical-Layer Analysis", *Proceedings of the Conference on Design, Automation and Test Europe*, 2013, pp. 1589–1594.

[25] J. T. Bessette and D. Ahn, "Vertically Stacked Microring Waveguides for Coupling between Multiple Photonic Planes", *Optics Express*, vol. 21, 2013, pp. 13580–13591.

[26] R. Morris, A. K. Kodi and A. Louri, "3D-NoC: Reconfigurable 3D Photonic On-Chip Interconnect for Multicores", *IEEE 30th Int. Conf. Computer Design (ICCD)*, pp. 413–418, 2012.

[27] D. G. Rabus, *Integrated Ring Resonators*, Springer, 2007.

[28] F. Xia, L. Sekaric and Y. Vlasov, "Ultracompact Optical Buffers on a Silicon Chip", *Nature photonics*, vol. 1, 2007, pp. 65–71.

[29] Y. Vlasov, W. M. Green and F. Xia, "High-Throughput Silicon Nanophotonic Wavelength-Insensitive Switch for On-Chip Optical Networks", *Nature photonics*, vol. 2, 2008, pp. 242–246.

[30] B. G. Lee, A. Biberman, N. Sherwood-Droz, C. B. Poitras, M. Lipson and K. Bergman, "High-Speed 2×2 Switch for Multiwavelength Silicon-Photonic Networks-On-Chip", *Journal of Lightwave Technology*, vol. 27, 2009, pp. 2900–2907.

Received 22 January 2018

Mohammad Reza Mokhtari received BS degree in electronics engineering from Urmia University and MSc Nanophotonics Engineering from the University of Tabriz, Iran. His research interests are optoelectronics devices and optical interconnects.

Hamed Baghban received his BS, MS, and PhD degrees in electronics engineering (Optical Integrated Circuits) from the University of Tabriz, Tabriz, Iran, in 2005, 2008, and 2011, respectively. He is currently an academic staff member (associate professor) of the Nanoelectronics Engineering Department, School of Engineering-Emerging Technologies, University of Tabriz, and his research interests include semiconductor lasers and amplifiers.

Hadi Soofi received his BS, MS, and PhD degrees in electronics engineering (Optical Integrated Circuits) from the University of Tabriz, Tabriz, Iran, in 2006, 2009, and 2013, respectively. He is currently an academic staff member (assistant professor) of the Nanoelectronics Engineering Department, School of Engineering-Emerging Technologies, University of Tabriz, and his research interests include organic light emitting diodes and optical modulators.